

Predicting Severity of COVID-19 From Patients' Chest CT Images Using Self-Supervised Image Segmentation Approaches

Daryl Fung, PingZhao. Hu, Carson Leung, Qian Liu, Judah Zammit

University of Manitoba, MB, Canada

ABSTRACT COVID-19 is the new outbreak of a contagious disease that infects the lungs. Currently, no vaccines or antiviral medicines exist for COVID-19 as COVID-19 is a newly infectious disease that was first discovered around December 2019. As COVID-19 is a very contagious disease, cases appear faster than the amount of test kit available. Currently, the most common testing used is PCR(Polymerase Chain Reaction) test. These test samples are sent to a centralized lab for analysis which would take several days for the test results to be available. Due to the exponential rate of infections, the limited amount of test kits, and the long wait time for the test results to be available, many infected patients are unable to get tested and receive treatments. An alternative approach to test for COVID-19 patients is through computerized tomography (CT) scan of the lungs. CT scan can drastically reduce the time taken for test results to be available and this could speed up the testing time as well as the limiting number of testing kits available. We will propose a deep learning architecture that can evaluate different segmentation of the lungs from CT images to detect if a patient is infected with COVID-19 so that we can reduce the amount of time taken to carry out testing to determine if patients are infected with COVID-19. In addition, we will calculate the severity of the lungs affected by the disease from the CT images. The lungs will be subdivided into different regions, a calculation of the severity of each region of the lungs will be carried out through evaluation of CT severity score (CT-SS) or Dice Similarity Coefficient (DSC).

INDEX TERMS Deep Learning, REMOVE THIS: TODO: update abstract, add multi-seg figure, add severity score performance

IMPACT STATEMENT The authors should include here a significance statement of no more than 30 words. The statement should summarize the main findings of the research work reported in the manuscript.

I. INTRODUCTION

COVID-19 is a newly identified disease that is very contagious and has been rapidly spreading across different countries around the world. The virus that was first identified in Wuhan has now infected more than 3.5 million people around the whole world and causes more than 245,000 deaths. Common symptoms from COVID-19 are fever, dry cough, but in more serious cases, patients can experience difficulty in breathing. As more people are infected, communities that have been in close contact with infected patients are getting tested for COVID-19. The test used to carry out the test for COVID-19 uses PCR(Polymerase Chain Reaction) test which could take several days for the test results to be available as the test samples are sent to a centralized lab for analysis and can be time consuming. There is a limited number of supplies of PCR tests which is a bottleneck for testing to be efficient. Several alternative methods have been considered to test patients that are COVID-19 positive including CT scan of the lungs. CT scans of the lungs are faster and easier to detect COVID-19 presence in patients. As the number of infected patients increases exponentially, it can be hard to provide testing scans for patients because of the limited number of doctors. It is recommended that Artificial Intelligence systems are used to analyse the CT scans of lung patients to determine the severity of COVID-19 and monitor the disease progression as well as

to compensate for the high number of patients. Specifically, we propose using deep learning to analyze and create a pixel-level segmentation of CT scan images of patients' lungs to determine the severity of COVID-19 in their lungs. In order to obtain the severity score, the model is first trained to segment the infected region of the lungs. Then, the severity score will be calculated by calculating the overlapping ratio between the segmented region for infected regions and the parenchyma of the lungs.

II. RELATED WORKS

There are several works that have been proposed to create image segmentation for CT scan lung images of COVID-19 positive patients. They have demonstrated effective solutions using deep neural networks to accurately predict if a patient has COVID-19 positive or negative.

A study has been conducted that uses multiple models for different tasks where the study uses both classification and image segmentation tasks for COVID-19 detection through multi-tasks learning. The study uses Inception Residual Recurrent Neural Network (IRRCNN) for the classification of COVID-19 detection and uses NAbLA-Net (NABLA-N) network for infected region segmentation for X-ray and CT images scan. [1] Transfer learning is used to retrain the IRRCNN model with samples to differentiate between COVID-19 positive samples and negative samples in the classification phase.

Mathematical Morphological approaches are implemented for selecting appropriate contours for chest region selection in the segmentation phase with NABLA-N network. Some classical imaging and adaptive threshold approaches are applied to extract the features to identify infected regions of COVID-19. They used a total number of 5,216 samples of which 3,875 samples are pneumonia and 1,341 samples are normal.

Another study [2] introduces a feature variation block and progressive atrous spatial pyramid pooling block using COVID-segNet, a high accuracy network that is able to create segmentation of COVID-19 infection from chest CT images. The network consists of an Encoder and a Decoder with residual skip connection connecting the encoder and the decoder at their respective layer, following the architecture of UNET [3]. Their main findings include the introduction of an FV block and a PASPP block. FV block consists of three branches - contrast enhancement branch, position sensitive branch, and identity branch. These branches can enable automatic change of parameters to display positions and boundaries of COVID-19. The PASPP block takes features extracted from the FV block to acquire semantic information with a variety of receptive fields. The dataset that they used consists of 21,658 labeled chest CT images, of which 861 CT images are confirmed COVID-19.

The paper above however conducted the study with a good amount of data samples to train the network to achieve a high performance. They obtained their dataset from hospitals through obtaining permission. We would like to create a network that does not require much labeled dataset to be able to achieve good performance. By doing this method, we could bring this network forward to detect new lung diseases when there are not much dataset available. Besides that, the paper is only able to recognize the presence of COVID-19 in a patient, but the papers could not quantify the severity of the disease.

While there is a limited number of public data samples available for CT COVID-19 lung images segmentation, it will not be feasible to train a network to achieve high performance. As there are not many COVID CT dataset that contains the segmentation ground-truth, we would like to train a network that contains the segmentation of the infected region so that the prediction results from our model will be more intuitive and easily comprehensible. There are a different number of research that resolve this issue. One method is to use semi-supervised learning to mitigate the problem of having a low number of data samples to improve the performance of deep neural networks. Instead of having to manually annotate the data, semi-supervised learning utilizes the unlabeled data samples to aid in the training for the network.

Deng Pin Fan et al. [14] used semi-supervised learning to enlarge the limited number of training samples for CT lung image segmentation. They developed a model called InfNet and semi-InfNet. The InfNet version of the model uses fully supervised method to predict the segmentation of the CT images for ground-glass opacities and consolidations. The model outputs 4 images of the segmentation for the CT lung images that contains either ground-glass opacities or consolidations with different image sizes. The segmentation of the different image sizes are resized to the same size as the ground truth

of the segmentation to compute the loss function. They also uses a edge loss to guide the model to predict the bounding area of the segmentation. To improve InfNet, they use semi-supervised by progressively enlarging the training dataset with unlabeled data using random sampling strategy. Specifically, they generate pseudo labels for unlabeled CT lung images. The advantage of using semi-supervised learning is that we can generate pseudo labels to increase the number of data samples. However, semi-supervised learning still require to generate new examples through the use of unlabeled CT lung images before being able to undergo its learning procedure. This requires the use of of unlabeled CT lung images to generate weakly labeled samples that are treated normally as labeled CT lung images to be fed into the network to train which could create a bias of distribution from the semi-supervised network weights.

Another study [27] uses Task-Based Feature Extraction Network (TFEN) and Covid-19 Identification Network (CIN). They propose to use task-specific feature extraction network that is tailored to CT lung images with three different classes: Healthy, pneumonia, and COVID-19 cases. They also mentioned that dataset for COVID-19 is still limited and there is not enough high quality dataset. They treat the task-specific feature extraction network as autoencoders and train the overall TFEN module to extract the relevant features from the CT images. Then, they use CIN to perform classification on the extracted features from the TFEN module. Due to the fact that by providing a person with limited CT images, they can easily detect the abnormal regions and differentiate between them very accurately by making use of prior information. This helped them develop a semi-supervised feature extraction network that allows obtaining the relevant prior information to perform the classification in order to mimic human behaviours. However, this study does not undergo segmentation of the CT lung images for better diagnosis of the CT lung images. It also does not provide the severity score of the CT lung image.

There is a study that predicts the severity score of COVID-19 on chest x-ray with deep learning [28]. They use a DenseNet model from the TorchXRayVision library as DenseNet models have been shown to predict Pneumonia well. They use a pre-training step to train the feature extraction layers and a task prediction layer. The pre-training step was used to generate a general representations of lungs and other CXRs that they would have unable to achieve from the small set of COVID-19 images available. They use a network that outputs 18 outputs of a representation of the image, 4 outputs that are a hand picked subset which contain the radiological findings (pneumonia, consolidation, lung opacity, and infiltration), and a lung opacity output. This study however did not use infected region segmentation to predict the severity score. They do not use self-supervised learning but pre-training steps to counter the limited data samples available for COVID-19.

III. PROBLEM STATEMENTS

Getting a high performance in deep neural networks requires an abundant amount of annotated samples. Performance can be drastically reduced if there are not enough data samples to compensate for the model's complexity. Likewise, complex

data distributions to learn require a higher model complexity to be able to fit the distribution with better performance. The related works utilizes semi-supervised learning to increase the amount of data samples to achieve higher performance. As pixel-level segmentation on CT images is a complex task, pixel-level segmentation requires a high model complexity to fit the distribution. Unfortunately, there is a limited number of publicly available COVID-19 dataset especially in the form of pixel-level segmentation. The limited number of samples available greatly reduce the performance of modeling complex distribution for pixel-level segmentation of CT scans lung images.

The related works does not also consider the severity of the lungs of patients as a result from COVID-19. We will propose a model and technique that utilizes self-supervised learning to mitigate the limited number of publicly available COVID-19 CT lung images samples as well as a method to calculate severity score of the segmented regions of CT lung images.

IV. METHODOLOGY

In this section, we will show the details of the self-supervised InfNet for imaging segmentation model including the network architecture, the data preprocessing steps, and the loss function. We will show how self-supervised InfNet helps to improve generalisation and performance of the model while having a limited number of data samples. We will also show the extension of our data preprocessing steps which further improves the performance of our model.

Supervised InfNet (Lung Infection Segmentation Network) will be used as our baseline to compare without using any semi-supervised learning algorithm. This is to show that the self-supervised learning method improves the performance of the baseline supervised learning InfNet for imaging segmentation. We will extend our work on supervised InfNet by adding self-supervised method to it.

We will not change the structure of the InfNet model and use the default parameters as included in their GitHub code. There will be two different types of the InfNet model - single InfNet and multi InfNet.

The single InfNet will create a single-labeled segmentation of the image for the infected region. The single InfNet predicts if the region is either ground-glass opacities or consolidations. It represents ground-glass opacities or consolidations as the same label. This means that the single InfNet will only predict the infected region without classifying them more specifically. The CT lung image is first passed into the initial convolutional layers of the single InfNet to extract the features of the CT lung image. Then, the features generated from the convolutional layer are fed into the partial decoder module, reverse attention module and the edge detection module. The edge detection module is to help the network with detection of the boundaries of the segmentation. The reverse attention and the partial decoder generates the segmentation of the infection regions of the CT lung images.

The prediction from the single InfNet represent the infected region and will act as a prior to be fed into the multi InfNet. The prior will be concatenate with the original CT image

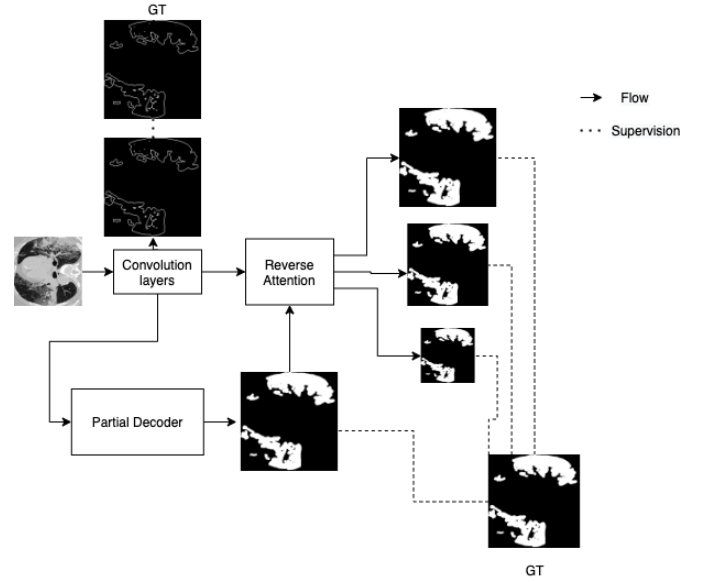


Fig. 1. Architecture of the supervised InfNet.

to be fed into the multi InfNet network. The multi InfNet network will be used to predict multiple-labeled segmentation. The multiple-labeled segmentation includes predicting the background, ground-glass opacities, and consolidations for the infected region. The multiple-labeled segmentation model will give each of the label a different value instead of grouping them as one as what the single-segmentation model does.

A. Self-supervised InfNet for imaging segmentation

We will propose using a self-supervised method to improve the performance of deep neural networks to create pixel-level segmentation for CT scan for lung images of COVID-19 patients. We will integrate self-supervised inpainting to pre-train our network. Since image inpainting is similarly related to image segmentation, we will integrate the pre-training steps as image inpainting for our image segmentation network.

The original InfNet model would generate 5 different predictions: the edge segmentation prediction, and the other 4 are segmentation of the infected regions but of different sizes. In order to utilise the ability of self-supervised method for InfNet segmentation, we generate masks to be fed into the InfNet model. The last convolution layer that outputs the prediction is not used for the self-supervised case. However, the last convolutional layer is replace with a different convolutional layer to reconstruct the image and the edge appropriately. Everything else is kept the same as the InfNet architecture. This way the network will learn meaningful representations of the CT images and we can use these meaningful representations to learn the segmentation of the infected regions of the CT lung images. After learning the self-supervised features for InfNet, the training continues as normal similar to the InfNet algorithm. The training will start with the weights trained using the self-supervised inpainting method. The last layer will be changed to its original layer instead of the replaced convolutional layer.

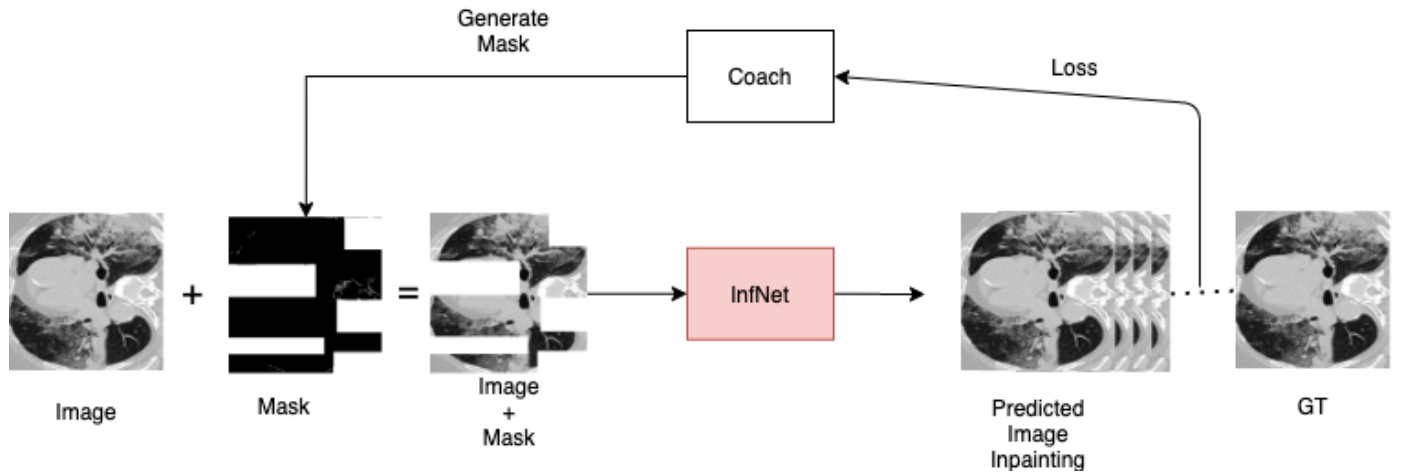


Fig. 2. The architecture of the coach network for self-supervised inpainting.

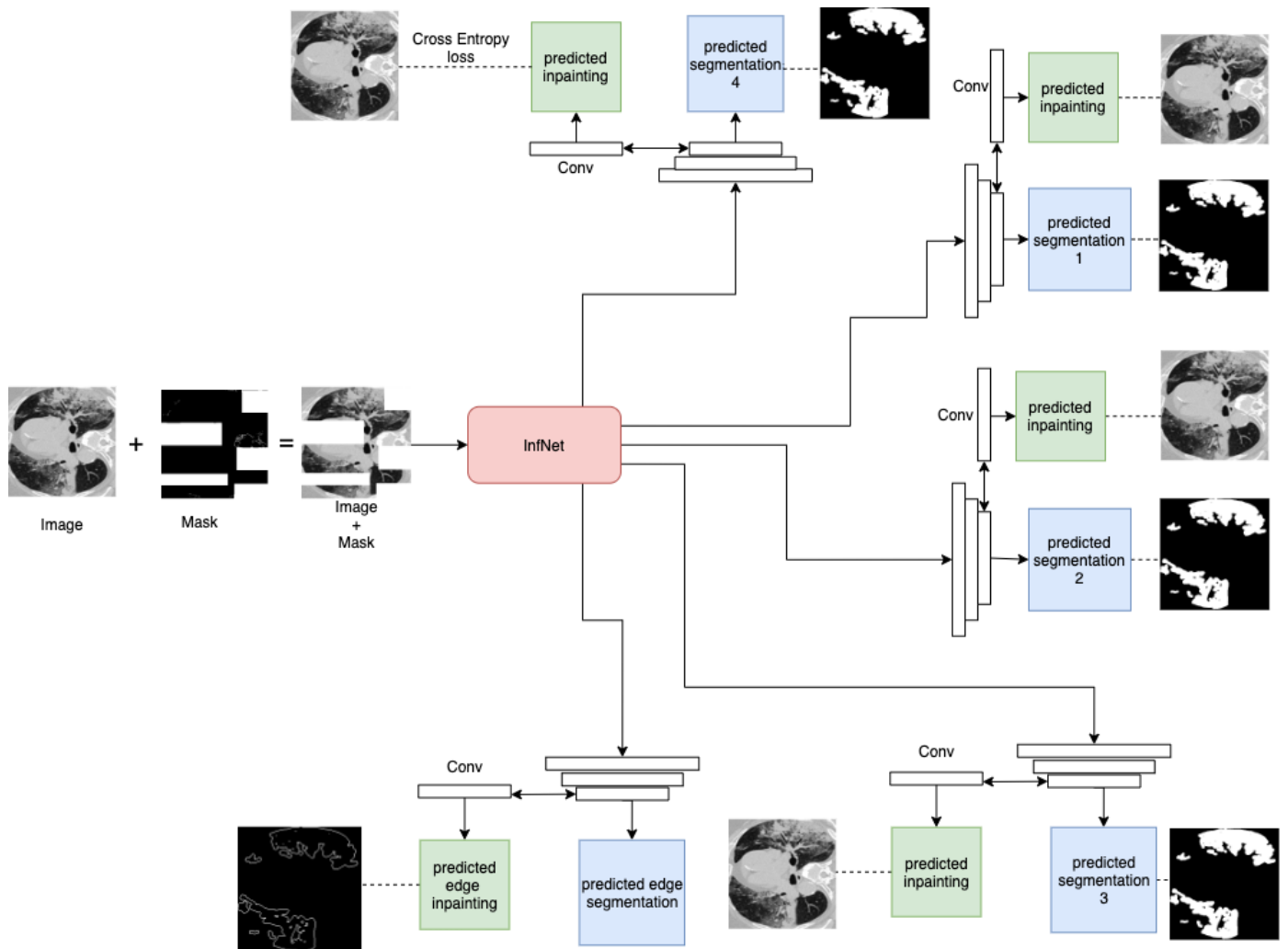


Fig. 3. The architecture of our self-supervised InfNet model.

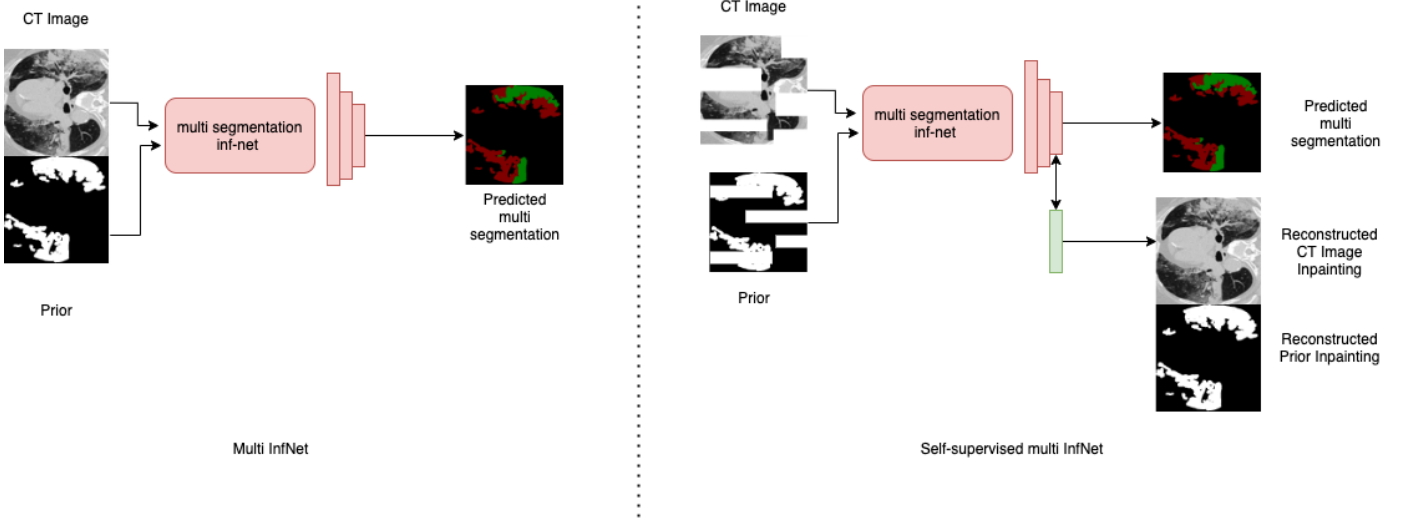


Fig. 4. The architecture of our self-supervised multi segmentation InfNet model. Highlighted green block is the difference between the original multi InfNet and our self-supervised multi InfNet.

By learning features from image inpainting, the model can learn more features that are related to image segmentation. As creating mask can be a complex task for the network to learn to inpaint, the mask can either be too complex for the network to start learning or too simple to be able to learn good representations. We will be using a coach network that increases the complexity of the masking of the CT images throughout the training of the network. The mask created will initially be relatively simple, once the network is able to predict the inpainting of the CT images with good performance, the coach will increase the complexity of the masking to reduce the performance of the network, similar to how Generative Adversarial Network (GAN) works. The loss for the coach network is constructed from the loss of the image inpainting from the InfNet. The coach network and the InfNet both work together as a MinMax algorithm. The InfNet will try and minimize the loss to generate better image inpainting while the coach network will try to increase the loss of the image inpainting through generating more complex masks. In the beginning, the masks generated by the coach network will be less complex. Through training of the coach network, as the InfNet gets better at predicting image inpainting, the coach network generates a more complex masks. The loss function for the coach network is:

$$L_{coach}(x) = 1 - L_{rec}(x \odot M) \quad (1)$$

where $M = C(x)$ which is created by the coach network. A constraint is apply to this loss function because the coach network would just create a mask that masks all region because no context information would be present for the network to learn and a maximum loss will be achieved. The constraint is:

$$\hat{B}(x) = B(x) - SORT(B(x))^{k|B(x)} \quad (2)$$

$$M = C(x) = \sigma(\alpha \hat{B}(x)) \quad (3)$$

The backbone, B, of the coach network has a similar network architecture with the model that inpaints the CT images. $SORT(B(x))$ sorts the features in descending order over the activation map. k represents the k^{th} elements in the sorted list and k helps to control the fraction of the image to be erased. The region that has scores lesser than the k^{th} element will be erased from the images. If k is 0.75 then 0.75 fraction of the images will not be erased. The score is scaled into a range of $[0, 1]$ using a sigmoid activation function. We keep $\alpha = 1$ while training the coach network.

After the self-supervision training is finished, the single segmentation InfNet would reuse the self-supervised single InfNet network weights to train normally on the segmentation of the CT lung images. Likewise, the multi InfNet network would reuse the weights that were trained during self-supervised multi InfNet training to train normally on the segmentation of the CT lung images.

The proposed self-supervised single-labeled segmentation InfNet network architecture can be seen in 3. The last layer for each output prediction is replace to a different linear activation layer. The linear activation layer will re-create the original image that is covered by the masks.

The proposed self-supervised multi-labeled segmentation InfNet network architecture is shown in 4. The changes in the architecture for the multi-labeled segmentation InfNet is similar to the single-labeled segmentation InfNet where the last layer of the layer is replace with a different linear activation layer to output the inpainting of the original image.

We will also implement different data augmentation that includes random cropping, rotation, and random cutout to increase the number of available annotated data samples and

Algorithm 1 Pseudo code for self-supervised with InfNet

Input: $D_{labeled} = [(inputImage_1, G_{t1}), \dots]$
for each epoch **do**
 for each coach step **do**
 $mask = M(x)$
 $maskedInput = mask \odot inputImage$
 $predictedImage = network(maskedInput), inputImage$
 $L_{rec} = CrossEntropy(predictedImage, inputImage)$
 $L_{coach}(x) = 1 - L_{rec}$
 update coach weights
 end for
 for each network step **do**
 $P_{labeled} = Preprocess(D_{labeled})$ // data aug
 $inpaintingOutput = network(P_{labeled})$
 $L_{rec} = CrossEntropy(InpaintingOutput, inputImage)$
 backpropagate and save network weights
 end for
end for
for each batch of $D_{labeled}$: **do**
 $P_{labeled} = Preprocess(D_{labeled})$
 $trainLoss = train(P_{labeled})$
 Backpropagate train loss
 $testLoss = test(P_{labeled})$
 save model weights, w .
end for

labels as well as improve the model generalization as the data samples for CT images from COVID-19 can be limited. We will show that proper data augmentation affect the performance of the model by a marginal amount.

The output of the single segmentation InfNet will include the edge of the segmentation and four single-labeled segmentation of the infected region of the CT lung images with different sizes as shown in 1. A loss will be calculated for each of the output from the single InfNet model. The first loss function is the loss edge, L_{edge} which guides the model in representing better segmentation boundaries. The other loss function is the segmentation loss, L_{seg} . The segmentation loss combines both the loss of Intersection over Union (IoU) and the binary cross entropy loss. The segmentation loss equation for the single InfNet is as follows:

$$L_{seg} = L_{IoU} + \lambda L_{BCE} \quad (4)$$

The λ is set to 1 for this experiment. The segmentation loss is adapted to all of the S_i predicted output where S_i are created from f_i such that $i = 3, 4, 5$.

The total loss function for the single InfNet model is then:

$$L_{total} = L_{seg}(G_t, S_g) + L_{edge} + \sum_{i=3}^5 L_{seg}(G_t, S_i) \quad (5)$$

The summation of the loss functions are calculated from the output of the three convolutional layers. G_t refers to the ground truth labels. S_g is the output from the parallel partial decoder to match with the ground truth label.

As for the multiple segmentation infected region InfNet. We also use the default model and hypermaters from the InfNet

code. We will however train the network without using any unlabeled images to be used as a supervised version. The CT lung images and prior (infected region) for the CT lung images are concatenate together before being fed into the multiple segmentation InfNet. The prior is generated from the single segmentation InfNet. The prior would contain the area of the infected region. However, the prior does not contain the labels for ground-glass opacities and consolidations. It just shows the infected regions. The multiple segmentation InfNet will label the CT lung images with background, ground-glass opacities, and consolidations. The architecture for multiple segmentation InfNet can be seen in 4. The loss function for the multiple segmentation InfNet is as follow:

$$L_{bce} = \frac{1}{N} \sum_{i=1}^N y_i \cdot \log(\hat{y}_i) + (1 - y_i) \cdot \log(1 - \hat{y}_i) \quad (6)$$

The loss function for multiple segmentation InfNet uses the binary cross-entropy between the predicted segmentation and the ground truth segmentation.

In order to improve the performance of the model and to aid in the generalisation, we determine to use self-supervised learning to learn good representations of the CT scan of lung images. Self-supervised learning generates auxiliary tasks from the labeled data samples. For instance, when undergoing data augmentation with rotation, we could train the network to predict if the images have been rotated 0 degree, 90 degree, 180 degree to learn representations of the images.

B. Estimation of Severity of COVID-19 from CT images

Once the network is able to predict the pixel-level segmentation of the CT scan images, we will use the pre-trained network to predict the segmentation of the infected region. We will then calculate the ratio between the segmentation of the infected region and the segmentation of the parenchyma in the ICTCF dataset. We use the algorithm provided by ICTCF to split the parenchyma from the CT lung images. We manually remove images that the parenchyma were not splitted properly. There were 6654 images from 1338 patients. After cleaning the dataset, we ended up with 6613 CT lung images with properly splitted parenchyma. We will then calculate the ratio between the infected lung region predicted by our network with the splitted parenchyma from the CT lung images to determine the severity of the lung. The CT lung images is first fed into the single SInfNet networks to generate the infected region. The infected region will have the shape of the CT lung images. Each pixel of the predicted infected region represent the amount of infection that range from 0 to 1 where 0 is not infected and 1 is highly infected. We will add the sum of the predicted infected region and divide it by the area of the parenchyma to obtain the ratio. The higher the ratio between the infected region and the splitted parenchyma, the higher the severity of the lung.

The equation for the ratio calculation is as follows:

$$Ratio = \frac{\hat{y}}{P} \quad (7)$$

Where P refers to the area of the parenchyma region and \hat{y} refers to the automatically segmented infected regions by the network.

We will compare our method against supervised and semi-supervised [13], [14] models trained on COVID-19 dataset. For comparing supervised learning, we will compare against the paper [13]. We will train and follow using the same network structure but change from supervised learning to self-supervised learning and compare the performance between supervised and self-supervised.

When comparing with the semi-supervised model, we determine that our model is successful if our model is able to reach close to or better than the performance of the semi-supervised model as semi-supervised model is able to obtain a higher amount of data samples by looking at both unannotated and annotated data samples while self-supervised model only have access to the annotated labels. A self-supervised learning method will create its own training annotated labels without any manual human labelling and trained without any unlabeled data samples. We will compare our method's performance against InfNet [14] which uses semi-supervised learning by generating pseudo labels from randomly selected unlabeled CT images.

Our method will be novel compare to the other methods mentioned as our method will be integrating both the segmentation of the CT lung images as well as the calculation of the severity score through calculation of the segmented infected lung areas.

V. EXPERIMENTS

Data split	Source	Segmented	Images	Patients
Training	Med-Seg	Yes	698	39
	ICTCF	No	6654	1338
Validation	Med-Seg	Yes	114	35
Testing	Med-Seg	Yes	117	35

TABLE I. This table shows the data distribution between the datasets that we use to evaluate our model on. Med-Seg refers to the COVID-19 CT Segmentation data set and ICTCF refers to the ICTCF data set.

A. Datasets

The dataset that we will be using is an integrative resource of chest computed tomography images and clinical features of patients with COVID-19 pneumonia (ICTCF) [23] which contains the severity score for each CT lung image and CT lung images from medical segmentation website [26].

ICTCF contains 127 types of clinical features and laboratory confirmed cases of COVID-19 from 1170 patients including the severity for the CT lung images. However, ICTCF dataset does not contain the segmentation labels for the ground-glass opacities and the consolidation in the CT lung images. In total, there are 6654 of CT lung images in ICTCF dataset. Originally, there were 1521 patients. However, some of the patients are missing CT lung images. We remove these patients that are missing CT lung images. After preprocessing the patients, the dataset was left with 1338 patients that contains CT lung images. The dataset can be found here: <http://ictcf.biocuckoo.cn/>.

As for the medical segmentation dataset, they contain ground truth label for the segmentation for ground-glass opacities and consolidation of the CT lung images but does not contain the severity score for the CT Lung images. The total amount of CT lung images contain in medical segmentation dataset is 932 CT lung images. We randomly assign the CT lung images into training set, validation set, and testing set of which the training set contains 698 CT lung images, the validation set contains 114 CT lung images, and the testing set contains 117 CT lung images.

The assignment of the dataset can be seen in I.

B. Experimental Settings

During the self-supervised image inpainting stage, we train the network for 2000 epochs. The network is trained for the first 200 epochs before we train the coach network for 200 epochs which increases the complexity of the masks generated. After that, we alternate in between training the self-supervised image inpainting and the coach network with 100 epochs in between. For every alternating between the training of the self-supervised image inpainting and the coach network, we set the learning rate to 0.1 at the start of the epoch, we set the learning rate to 0.01 at 40th epoch, we set the learning rate to 0.001 at 80th epoch, and 0.0001 at the 90th epoch. We use SGD as the optimizer for the self-supervised image inpainting. We set the momentum to 0.9 and the weight decay to 0.0005. As for the optimizer for the coach network, we use Adam optimizer with learning rate of 0.00001.

For the Single InfNet, we train the network for 500 epochs. We use Adam as the optimizer with learning rate of 0.0001.

For the Multi InfNet, we train the network for 500 epochs. We use SGD as the optimizer. The momentum is set as 0.7 and the learning rate is set as 0.01.

For the severity score calculation, there are several different labels obtained from ICTCF dataset for severity, The different severity are: *Regular*, *Mild*, *Control*, *Severe*, *Critically ill*. The assign the different labels with score ranging from 0 to 2. *Regular*, *Mild*, and *Control* are assign having a severity score of 0. *Severe* is assign having a severity score of 1. *Critically ill* is assign having a severity score of 2. We use the metrics provided by sklearn to calculate the F1 Score, Precision Score, and Recall Score for the severity score prediction. We use 'micro' as the averaging for the scores as provided by sklearn.

C. Data Augmentation

We used data augmentation to increase our data samples size. The data augmentation that we used includes *vertical flipping*, *horizontal flipping*, *random crop*, and *random cutout*. For the random cutout percentage, we experimented that 0.5 cDuring tutout of the CT lung images yield higher performance than the rest of the value. This is because entropy at 0.5 is the highest which could increase more variability of the images. Examples of the data augmentation can be seen in figure 6. The left column is the original CT lung images while the right column is the augmented CT lung images. The first row involves random cropping and random cutout. The second row involves random cropping and random cutout. The third row

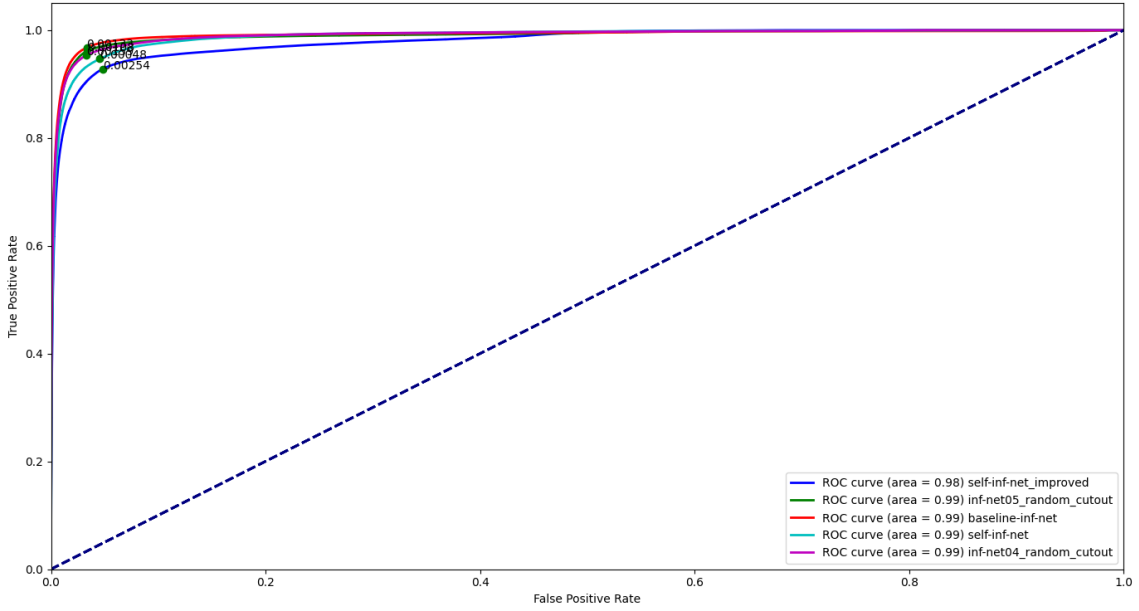


Fig. 5. ROC comparison of different networks.

Methods		F1	IoU	Recall	Precision	AUC
Single SInfNet	Mean	0.39	0.29	0.83	0.33	0.9909
	Error	± 0.059	± 0.053	$\pm \mathbf{0.069}$	± 0.057	± 0.032
Single SInfNet + data aug(0.4)	Mean	0.38	0.27	0.79	0.34	0.9903
	Error	± 0.054	± 0.045	± 0.071	± 0.055	± 0.017
Single SInfNet + data aug (0.5)	Mean	0.37	0.26	0.81	0.32	0.9893
	Error	± 0.054	± 0.045	± 0.072	± 0.050	± 0.021
Single Self-SInfNet	Mean	0.38	0.27	0.75	0.33	0.9883
	Error	± 0.056	± 0.049	± 0.077	± 0.053	± 0.010
Single Self-SInfNet + data aug	Mean	0.30	0.20	0.72	0.28	0.9795
	Error	$\pm \mathbf{0.050}$	$\pm \mathbf{0.039}$	± 0.085	$\pm \mathbf{0.045}$	$\pm \mathbf{0.006}$

TABLE II. Quantitative result for comparison between Single segmentation InfNet and self-supervised single segmentation InfNet in the test set.

involves random cropping and vertical flipping. The random cutout involves patching the image with colors of the same value of rgb. For instance, if the value of r is 10, then the value of g and b are also 10. If the value of r is 50, then the value of g and b are also 50.

VI. RESULTS

In this section, we will show the results of our experiments obtained. We will divide this section into two different subsections: Result for self-supervised InfNet and result for estimation of severity score.

A. Result for self-supervised InfNet

The result for our comparison between the baseline InfNet model and our self-supervised model can be seen in II, IV,

and V. The table is plotted with several metrics: dice, jaccard, sensitivity, specificity, and mean absolute error (MAE).

For the table that contains mean and error, the mean are calculated as:

$$mean = \frac{\sum_{i=1}^N Metric(\hat{y}_i, y_i)}{N} \quad (8)$$

Where Metric refers to either *Dice*, *Jaccard*, *Sensitivity*, *Specificity*, or *mean absolute error (MAE)*. N refers to the number of test data samples. The error is:

$$error = SE \times 1.96 \quad (9)$$

where SE is the standard error of the test data samples for the metric multiplied by 1.96. Note that Mean \pm Error is the 95% confidence interval.

We show several tables for our comparisons. II shows the result for the single segmentation InfNet. The single segmen-

Methods		Ground-Glass Opacity				Consolidation			
		F1	IoU	Recall	Precision	F1	IoU	Recall	Precision
SInfNet	Mean	0.38	0.27	0.58	0.41	0.29	0.22	0.61	0.31
	Error	± 0.054	± 0.042	± 0.065	± 0.058	± 0.078	± 0.068	± 0.099	± 0.084
SInfNet+ data aug(0.4)	Mean	0.35	0.25	0.58	0.38	0.3	0.23	0.62	0.32
	Error	± 0.056	± 0.043	± 0.072	± 0.058	± 0.08	± 0.069	± 0.102	± 0.084
SInfNet+ data aug(0.5)	Mean	0.34	0.24	0.59	0.35	0.4	0.32	0.55	0.49
	Error	± 0.055	± 0.042	± 0.072	± 0.057	± 0.098	± 0.087	± 0.115	± 0.106
SSInfNet	Mean	0.36	0.26	0.56	0.4	0.31	0.25	0.56	0.38
	Error	± 0.055	± 0.043	± 0.067	± 0.059	± 0.087	± 0.076	± 0.114	± 0.097
SSInfNet+ data aug	Mean	0.34	0.24	0.56	0.37	0.18	0.14	0.5	0.24
	Error	± 0.054	± 0.042	± 0.068	± 0.056	± 0.059	± 0.051	± 0.117	± 0.071

Methods		Background				Overall			
		F1	IoU	Recall	Precision	F1	IoU	Recall	Precision
SInfNet	Mean	1.0	0.99	0.99	1.0	0.55	0.5	0.73	0.57
	Error	± 0.002	± 0.003	± 0.002	± 0.002	± 0.044	± 0.038	± 0.055	± 0.048
SInfNet+ data aug(0.4)	Mean	0.99	0.99	0.99	1.0	0.55	0.49	0.73	0.56
	Error	± 0.002	± 0.003	± 0.002	± 0.002	± 0.046	± 0.038	± 0.059	± 0.048
SInfNet+ data aug(0.5)	Mean	1.0	0.99	0.99	1.0	0.58	0.52	0.71	0.61
	Error	± 0.002	± 0.003	± 0.002	± 0.002	± 0.052	± 0.044	± 0.063	± 0.055
SSInfNet	Mean	1.0	0.99	1.0	1.0	0.56	0.5	0.71	0.59
	Error	± 0.002	± 0.003	± 0.002	± 0.002	± 0.048	± 0.041	± 0.061	± 0.053
SSInfNet+ data aug	Mean	1.0	0.99	1.0	1.0	0.51	0.46	0.68	0.53
	Error	± 0.002	± 0.003	± 0.002	± 0.002	± 0.038	± 0.032	± 0.062	± 0.043

TABLE III. Quantitative result of Ground-glass Opacities & Consolidation on the test data set. Prior is obtained from the single segmentation InfNet

Methods		Ground-Glass Opacity			
		F1	IoU	Recall	Precision
SInfNet	Mean	0.38	0.27	0.58	0.41
	Error	± 0.054	± 0.042	± 0.065	± 0.058
SSInfNet	Mean	0.36	0.26	0.56	0.4
	Error	± 0.055	± 0.043	± 0.067	± 0.059

Methods		Consolidation			
		F1	IoU	Recall	Precision
SInfNet	Mean	0.29	0.22	0.61	0.31
	Error	± 0.078	± 0.068	± 0.099	± 0.084
SSInfNet	Mean	0.31	0.25	0.56	0.38
	Error	± 0.087	± 0.076	± 0.114	± 0.097

Methods		Overall			
		F1	IoU	Recall	Precision
SInfNet	Mean	0.55	0.5	0.73	0.57
	Error	± 0.044	± 0.038	± 0.055	± 0.048
SSInfNet	Mean	0.56	0.5	0.71	0.59
	Error	± 0.048	± 0.041	± 0.061	± 0.053

TABLE IV. Quantitative result of Ground-glass Opacities & Consolidation on the test data set. Prior is obtained from the single segmentation InfNet

tation InfNet does not segment between ground-glass opacities or consolidation. The single segmentation will segment and

represent all infected region as one. We can see that self-supervise can improve on the generalisation and consistency

Methods		Ground-Glass Opacity				Consolidation			
		F1	IoU	Recall	Precision	F1	IoU	Recall	Precision
SInfNet	Mean	0.87	0.81	0.87	0.9	0.47	0.39	0.68	0.55
	Error	± 0.041	± 0.049	± 0.043	± 0.042	± 0.102	± 0.093	± 0.103	± 0.111
SInfNet+ data aug(0.4)	Mean	0.86	0.81	0.87	0.91	0.58	0.47	0.64	0.74
	Error	± 0.048	± 0.058	± 0.052	± 0.04	± 0.096	± 0.092	± 0.108	± 0.095
SInfNet+ data aug(0.5)	Mean	0.86	0.81	0.88	0.9	0.53	0.44	0.62	0.69
	Error	± 0.045	± 0.055	± 0.05	± 0.042	± 0.108	± 0.099	± 0.118	± 0.108
SSInfNet	Mean	0.86	0.8	0.87	0.89	0.55	0.46	0.67	0.68
	Error	± 0.041	± 0.051	± 0.044	± 0.039	± 0.106	± 0.101	± 0.116	± 0.108
SSInfNet+ data aug	Mean	0.82	0.74	0.82	0.86	0.27	0.22	0.61	0.31
	Error	± 0.046	± 0.053	± 0.048	± 0.04	± 0.077	± 0.067	± 0.117	± 0.088
Methods		Background				Overall			
		F1	IoU	Recall	Precision	F1	IoU	Recall	Precision
SInfNet	Mean	1.0	1.0	1.0	1.0	0.78	0.73	0.85	0.82
	Error	± 0.0	± 0.0	± 0.0	± 0.0	± 0.047	± 0.048	± 0.049	± 0.051
SInfNet+ data aug(0.4)	Mean	1.0	1.0	1.0	1.0	0.81	0.76	0.84	0.88
	Error	± 0.0	± 0.0	± 0.0	± 0.0	± 0.048	± 0.05	± 0.053	± 0.045
SInfNet+ data aug(0.5)	Mean	1.0	1.0	1.0	1.0	0.8	0.75	0.83	0.86
	Error	± 0.0	± 0.0	± 0.0	± 0.0	± 0.051	± 0.051	± 0.056	± 0.05
SSInfNet	Mean	1.0	1.0	1.0	1.0	0.8	0.75	0.85	0.86
	Error	± 0.0	± 0.0	± 0.0	± 0.0	± 0.049	± 0.05	± 0.054	± 0.049
SSInfNet+ data aug	Mean	1.0	1.0	1.0	1.0	0.69	0.65	0.81	0.72
	Error	± 0.0	± 0.0	± 0.0	± 0.0	± 0.041	± 0.04	± 0.055	± 0.043

TABLE V. Quantitative result of Ground-glass Opacities & Consolidation on the test data set. Prior is obtained from the test set.

Method	F1 Score	Precision	Recall
SInfNet	0.28	0.28	0.28
SInfNet+data aug(0.4)	0.61	0.61	0.61
SInfNet+data aug(0.5)	0.42	0.42	0.42
Self SInfNet	0.55	0.55	0.55
Self SInfNet+data aug	0.62	0.62	0.62

TABLE VI. Table shows the result of severity score prediction on CT lung images using segmentation.

on predicting on the different CT lung images as they perform the best in terms of the error range. Even though the baseline single SInfNet performance have better mean values for dice, jaccard, AUC, and sensitivity, the self-supervised and the data augmentation approach helps to create robustness and consistency in the model itself to better handle outliers. We can see the results of the single segmentation in 7. We can see that the baseline single SInfNet overestimated the infected region of an outlier in the segmentation result in the figure in the last row. The baseline single SInfNet even with added data augmentation predicted some infected region in the CT lung images when the ground truth does not contain any infected region. The self-supervised SInfNet did a better job at predicting outlier's where its prediction is more closely related to the ground truth than the baseline single SInfNet.

IV shows the result for the comparison between multiple segmentation InfNet. As the multiple segmentation InfNet

requires a CT lung image concatenate with a prior as input where the prior is the segmentation of the infected region of the CT lung without considering the location of ground-glass opacities or consolidation. The prior represents the infected region as a whole. For the result of this table, the prior is obtained by running prediction of the single segmentation InfNet on the CT lung images of the test set. Then the prior is fed together with the CT lung image from the test set into the multiple segmentation InfNet to obtain the result. As the baseline InfNet achieves the best performing single InfNet, we use the prediction obtained from the baseline InfNet as prior to be fed into the multi segmentation InfNet with the CT lung images. Even though the baseline multiple segmentation InfNet has the best performance, self-supervised creates a more consistent and robust network to outliers. We can see the segmentation result in 8. The self-supervised with data augmentation does not seem to improve the performance on the self-supervised multi InfNet. However, it does reduce the difference in the error variation between different CT lung images. This means that data augmentation helps to cover a wide variety of CT lung images to create a more consistent prediction. Similar to the single segmentation network, the self-supervised are able to predict output that is more closely related to the ground-truth when fed with CT lung images with different distribution as shown in the last row of the figure.

V Shows the result for the comparison between multiple segmentation InfNet. The prior fed into the multiple segmen-

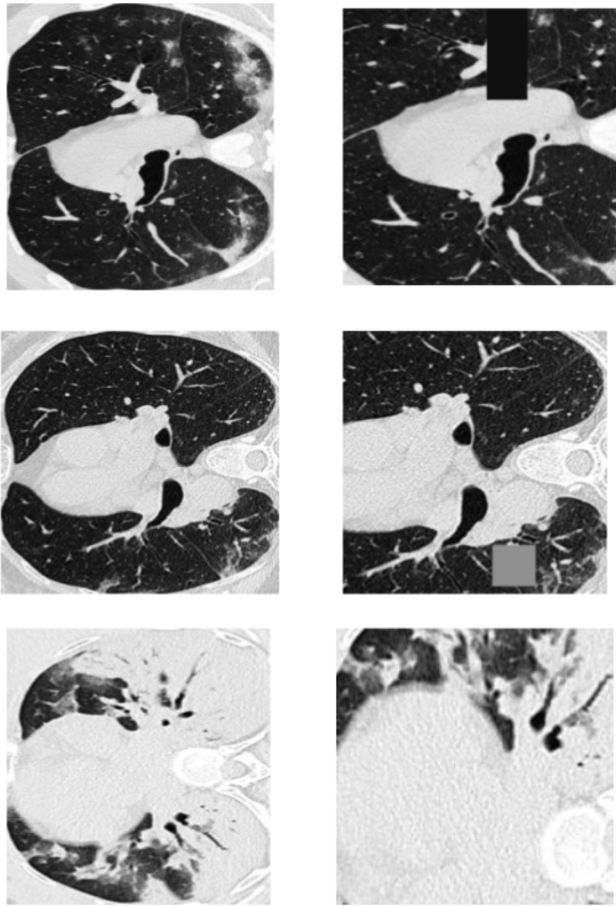


Fig. 6. Example of data augmentation on the CT lung images.

tation InfNet for this result is the ground truth prior obtained from the test set. For the result of this table, the prior is obtained from the test set. The prior is therefore the ground-truth of the segmentation of the single SInfNet. We can see from the table that the multi self SInfNet is the best performing network compare to the rest of the network. We can see that data augmentation improves the consistency of the network. However, data augmentation does not necessarily improve the performance of the network. Data augmentation makes a network more robust to outliers but does not necessarily improve the performance of the network in CT lung images. The self-supervised multi SInfNet achieves the best error variation compared to the other networks. We can see the figure of the comparison between different multi segmentation SInfNet with strong prior (Priors that are obtained from the test dataset) in 9.

B. Result for estimation of severity score

VI shows the result of the severity score with different networks. We can see that having data augmentation improves the performance of the baseline InfNet in severity calculation. It achieves an F1 score of 0.61, an amount of more than two times the performance of baseline InfNet network. Enabling a higher value of random cutout in the data augmentation seems

to reduce the performance of the severity score calculation by a marginal amount. The result of baseline InfNet with data augmentation where the random cutout is set to 0.5 have an F1 score of 0.42 with severity calculation. As having a higher random cutout value improves the network capacity to predict the image inpainting of the CT lung images, the capacity for the network to generalize to other information is lost. Adding self-supervised learning to the baseline InfNet model improves the network performance to 0.55, the performance is still lower than the baseline InfNet with data augmentation but it is two times the performance of baseline InfNet. Our self-supervised InfNet with added data augmentation yields the best performing result. The self-supervised InfNet with added data augmentation achieves a result of 0.62. The combination of self-supervised learning and data augmentation helps the InfNet model to generalise to different tasks as both technique aids the model in learning detailed information about CT lung images and a more diverse CT lung images distribution. Even though self-supervised InfNet does not improve the performance of predicting the multiple segmentation of the CT lung images on the same dataset, when a dataset with different distribution is introduced and the task is different, self-supervised InfNet combined with data augmentation beats the performance of the other networks.

VII. CONCLUSION

A conclusion section is required. Although a conclusion may review the main points of the paper, do not replicate the abstract as the conclusion. A conclusion might elaborate on the major findings and significance of the work or suggest applications and extensions. Do not exceed 300 words for the conclusion section.

REFERENCES

- [1] Alom, MZ., Rahman, MMS., Nasrin, MS., Taha, TM., Asari, VK. *COVID-MTNet: COVID-19 Detection with Multi-Task Deep Learning Approaches*. arXiv:2004.03747, 2020.
- [2] Yan, Q., Wang, B., Gong, D., et al. *COVID-19 Chest CT Image Segmentation – A Deep Convolutional Neural Network Solution*. arXiv:2004.10987, 2020.
- [3] Ronneberger, O., Fischer, P., and Brox, T. *U-net: Convolutional networks for biomedical image segmentation*. In MICCAI, pages 234–241. Springer, 2015. 2
- [4] Kalluri, T., Varma, G., Chandraker, M., and Jawahar, CW. *Universal semi-supervised semantic segmentation*. CoRR, abs/1811.10323, 2018.
- [5] Misra, I., and van der Maaten, L. *Self-supervised learning of pretext-invariant representations*. arXiv preprint arXiv:1912.01991, 2019.
- [6] Chen, T., Kornblith, S., Norouzi, M., and Hinton, G. *A simple framework for contrastive learning of visual representations*. arXiv:2002.05709, 2020.
- [7] Newell, A., Deng, J. *How Useful is Self-Supervised Pretraining for Visual Tasks?* arXiv:2003.14323, 2020.
- [8] Novosel, J., Viswanath, P., and Arsenali, B. *Boosting Semantic Segmentation With Multi-Task Self-Supervised Learning for Autonomous Driving Applications*. In Proc. of NeurIPS - Workshops, pages 1–11, Vancouver, BC, Canada, Dec. 2019.
- [9] Kahl, F. *“Fine-grained segmentation networks: Self-supervised segmentation for improved long-term visual localization,”* in Proceedings of the IEEE International Conference on Computer Vision, 2019, pp. 31–41.
- [10] Chang, YC., Yu, CJ., Chang, SC., et al. *Pulmonary sequelae in convalescent patients after severe acute respiratory syndrome: evaluation with thin-section CT*. Radiology 2005; 236(3):1067-1075.
- [11] Yang, R., Li, X., Liu, H., Zhen, Y., Zhang, X., Xiong, Q., et al. *Chest CT Severity Score: An Imaging Tool for Assessing Severe COVID-19*. Radiol Cardiothorac Imaging. 2020;2(2):e200047.

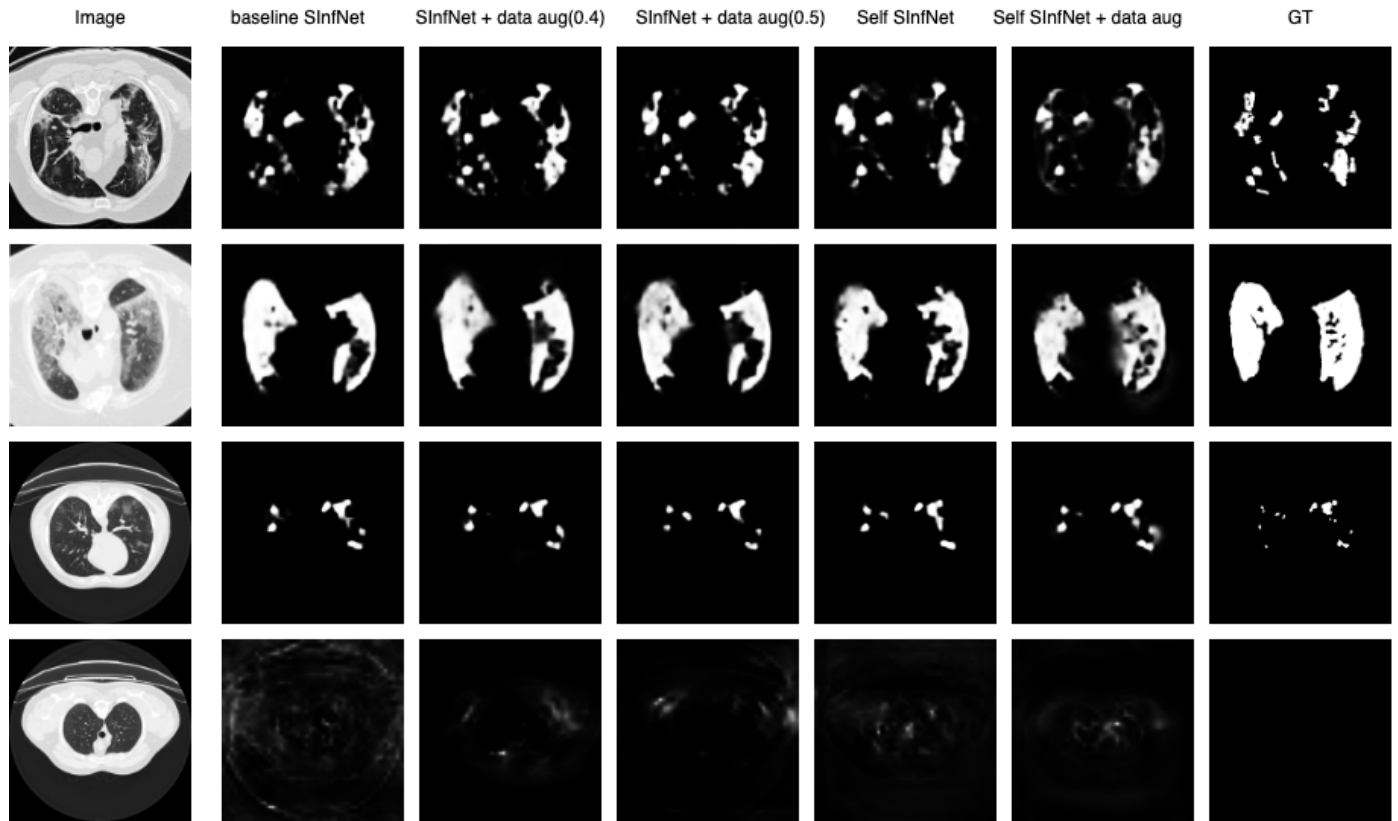


Fig. 7. Comparison of single segmentation between different networks.

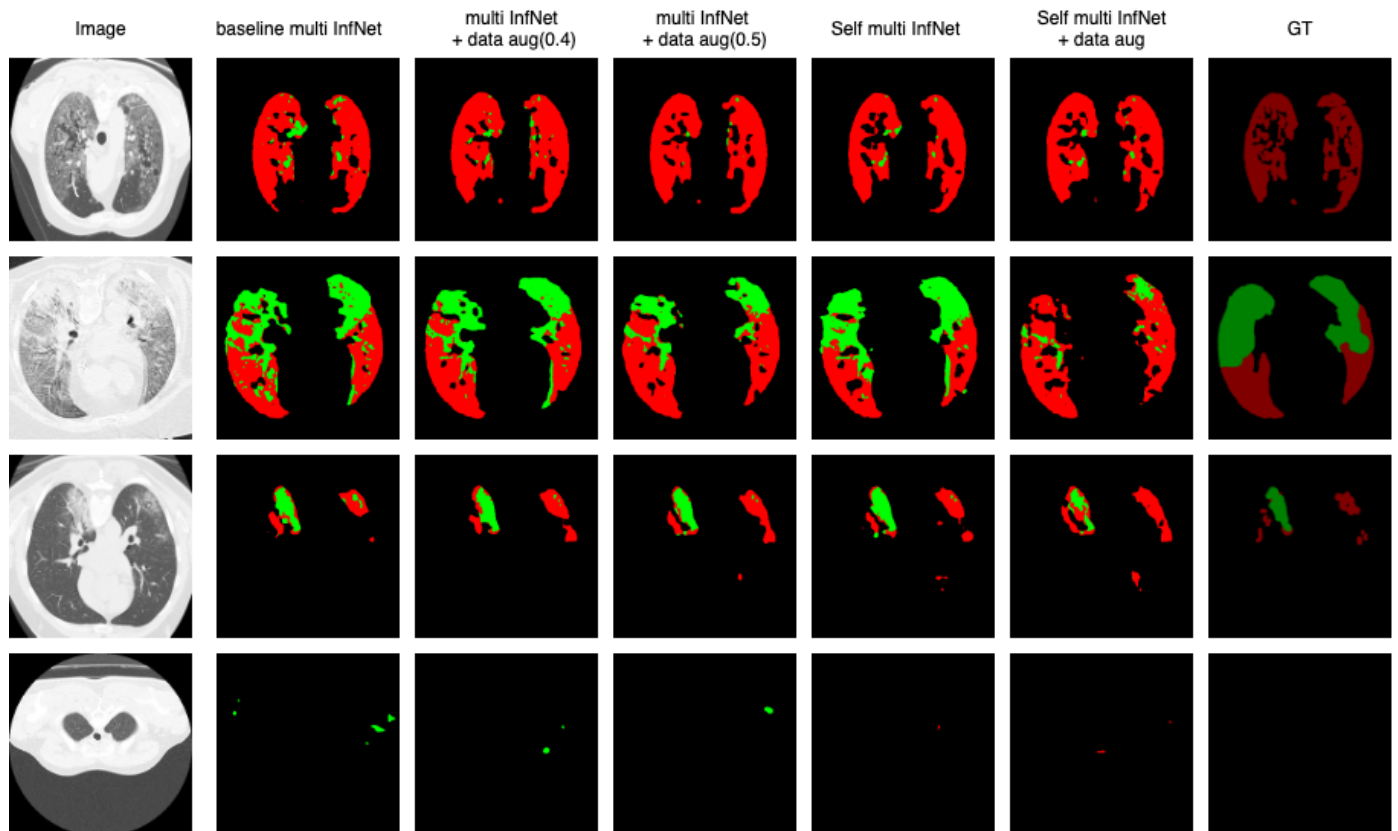


Fig. 8. Comparison of multi segmentation between different networks with prior generated from single InfNet.

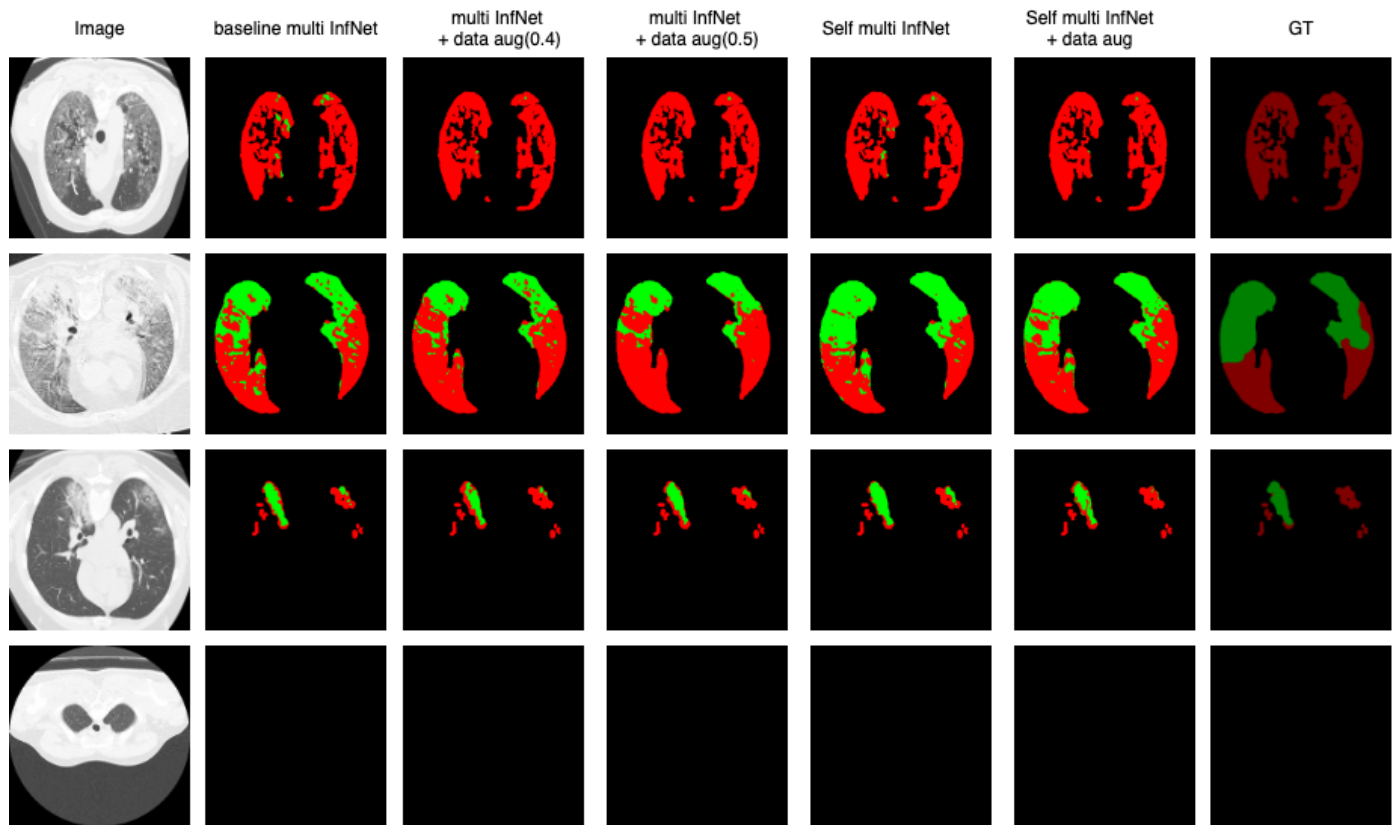


Fig. 9. Comparison of multi segmentation between different networks with prior from Test Set.

- [12] Shan, F., Gao, Y., Wang, J., Shi, W., Shi, N., Han, M., Xue, Z., and Shi, Y. *Lung Infection Quantification of COVID-19 in CT Images with Deep Learning*. arXiv preprint arXiv:2003.04655, 1-19, 2020.
- [13] Yan, Q., Wang, B., Gong D., et al. *COVID-19 Chest CT Image Segmentation – A Deep Convolutional Neural Network Solution*. arXiv preprint arXiv:2004.10987, 2020.
- [14] Fan, DP., Zhou, T., Ji, GP., et al. *Inf-Net: Automatic COVID-19 Lung Infection Segmentation from CT Scans*. arXiv preprint arXiv:2004.14133v2, 2020.
- [15] Alexander Kolesnikov, Xiaohua Zhai, and Lucas Beyer. *Revisiting self-supervised visual representation learning*. In Conference on Computer Vision and Pattern Recognition (CVPR), 2019.
- [16] Trinh, TH., Luong, MT., and Le, QV. *Selfie: Self-supervised pretraining for image embedding*. arXiv preprint arXiv:1906.02940, 2019.
- [17] Frinken, V., Zamora-Martinez, F., Espana-Boquera, S., Castro-Bleda, M. J., Fischer, A., and Bunke, H. (2012). *Long-short term memory neural networks language modeling for handwriting recognition*. In Pattern Recognition (ICPR), 2012 21st International Conference on, pages 701–704. IEEE.
- [18] LeCun, Y., Haffner, P., Bottou, L., and Bengio, Y. *Object recognition with gradient-based learning*. In Shape, contour and grouping in computer vision, pages 319–345. 1999.
- [19] Kingma, Diederik, P. and Welling, M. *Auto-Encoding Variational Bayes*. In The 2nd International Conference on Learning Representations (ICLR), 2013.
- [20] Goodfellow IJ., Pouget-Abadie, J., Mirza, M., Xu, B., Warde-Farley, D., Ozair, S., Courville, AC., and Bengio, Y. *Generative adversarial nets*. In Proceedings of NIPS, pages 2672– 2680, 2014.
- [21] Zhao, JY., Zhang, YC., He, XH., Xie, PT. *COVID-CT-Dataset: a CT scan dataset about COVID-19*. arXiv preprint arXiv: 2003.13865, 2020.
- [22] Cohen, JP., Morrison, P., and Dao, L. *COVID-19 Image Data Collection*. arXiv preprint arXiv: 2003.11597, 2020. <https://github.com/ieee8023/covid-chestxray-dataset>.
- [23] Ning, Lei, WS., Yang SJ., et al. (2020). *iCTCF: an integrative resource of chest computed tomography images and clinical features of patients with COVID-19 pneumonia*. 10.21203/rs.3.rs-21834/v1.
- [24] Zhang, K., Liu, XH., Shen, J., et al. *Clinically Applicable AI System for Accurate Diagnosis, Quantitative Measurements and Prognosis of COVID-19 Pneumonia Using Computed Tomography*. DOI: 10.1016/j.cell.2020.04.045.
- [25] Singh, S., Batra, A., Pang, G., Torresani, L., Basu, S., Paluri, M., and Jawahar, C. V. *Self-supervised feature learning for semantic segmentation of overhead imagery*. In BMVC, 2018.
- [26] *COVID-19 CT segmentation dataset*. Retrieved from <http://medicalsegmentation.com/covid19/>.
- [27] Khobahi, S., Agarwal, C., Soltanalian, M. *CoroNet: A Deep Network Architecture for SemiSupervised Task-Based Identification of COVID-19 from Chest X-ray Images*. In medRxiv, 2020.
- [28]] Cohen, J. P., Dao, L., Morrison, P., Roth, K., Bengio, Y., Shen, B., Abbasi, A., Hoshmand-Kochi, M., Ghassemi, M., Li, H., Duong, T. Q. *Predicting covid19 pneumonia severity on chest x-ray with deep learning*, arXiv preprint arXiv:2005.11856.